doi.org/10.36721/PJPS.2026.39.11.308.1

Bone marrow mesenchymal stem cells relieve rheumatoid arthritis by blocking JAK/STAT and TLR-4/NF-κB pathways

Shilin Lian#, Xiao Ma#, Yichen Meng and Xuhui Zhou*
Department of Orthopedics, Shanghai Changzheng Hospital, Naval Medical University, Shanghai, 200003, China

Abstract: **Background**: Rheumatoid arthritis (RA) is a chronic autoimmune disorder characterized by synovial inflammation and joint destruction. Bone marrow mesenchymal stem cells (BMSCs) have shown therapeutic potential in RA, but the underlying mechanisms remain poorly understood. **Objectives**: To investigate the effects of BMSCs on human RA fibroblast-like synovial MH7A cells and complete Freund's adjuvant (CFA)-induced arthritis in rats and to explore the involvement of the JAK/STAT and TLR-4/NF-κB signaling pathways. **Methods**: BMSCs were isolated and co-cultured with MH7A cells. CFA-induced arthritis rat models were established. MH7A cell viability, inflammatory cytokine levels, paw withdrawal thermal latency (PWTL), gait parameters and the expression of JAK/STAT and TLR-4/NF-κB pathway-related genes and proteins were assessed. **Results**: *In-vitro*, BMSC co-culture significantly inhibited MH7A cell viability and reduced TNF-α, IL-6 and IL-8 levels. BMSC treatment also downregulated the expression of JAK2, p-JAK2, STAT3, p-STAT3, TLR4, P65 and p-P65 in MH7A cells. *In-vivo*, BMSC administration improved PWTL and gait parameters, reduced serum inflammatory cytokine levels and suppressed the expression of JAK/STAT and TLR-4/NF-κB pathway components in synovial tissues of CFA-induced arthritic rats. **Conclusion**: BMSCs alleviate RA by inhibiting inflammatory responses *in vitro* and *in vivo* and the underlying mechanism may involve blockade of the JAK/STAT and TLR-4/NF-κB signaling pathways.

Keywords: Bone marrow mesenchymal stem cells; JAK/STAT signaling pathway; Rheumatoid arthritis; Synovial cells; TLR-4/NF-κB pathway

Submitted on 05-01-2025 – Revised on 02-04-2026 – Accepted on 09-04-2026

INTRODUCTION

Rheumatoid arthritis (RA) is an inflammatory, chronic autoimmune and disabling disorder and shows complex pathogenesis with an interaction of environmental and genetic factors (Wen *et al*., 2023). Common manifestations of RA include cartilage damage, synovial inflammation and synovial hyperplasia, which may trigger an abnormal immune response and lead to progressive destruction of articular cartilage and bone (Jing *et al*., 2023). Synovial fibroblasts (MH7A) are an important part of synovial tissue and can induce inflammation by secreting various inflammatory factors (Zhang *et al*., 2025). At present, the pathogenic factors and pathological mechanisms of arthritis are still not completely clear. Clinical treatment can only reduce patients' symptoms and delay disease progression (Pan *et al*., 2024). Celastrol (Cel), a next-generation non-steroidal anti-inflammatory analgesic, has been shown to regulate Th1 and Th2 cells, macrophages, fibroblasts and endothelial cells by affecting various signaling proteins, thereby exerting therapeutic effects in RA (Chen *et al*., 2025). However, although Cel shows a good anti-inflammatory effect on RA, adverse reactions may occur after long-term use (Zhang *et al*., 2025). Therefore, seeking new treatment modalities are urgent.

In recent years, with the rise of cell therapy, the use of mesenchymal stem cells for the treatment of refractory arthritis has attracted significant attention. Bone marrow mesenchymal stem cells (BMSCs) are important adult pluripotent progenitor cells with low immunogenicity and a stable genetic background and can differentiate into bone, cartilage and adipose tissue. Previous studies have shown that BMSCs exert therapeutic effects in Freund's complete adjuvant (CFA)-induced knee osteoarthritis rat models (Deng *et al*., 2023; Guzel Erdogan *et al*., 2025), but the underlying mechanisms remain to be further elucidated. Notably, the activation of several signaling pathways is closely linked to RA progression. The JAK/STAT signaling pathway is a ubiquitously expressed intracellular signal transduction pathway that mediates various biological functions, such as cell proliferation and immunoregulation (Hu *et al*., 2023). Activation of the JAK/STAT pathway induced by pro-inflammatory cytokines has been identified as a key factor in maintaining the chronic inflammatory state that leads to synovial joint failure in RA (Kiełbowski *et al*., 2024). In addition, the anti-inflammatory effect of the TLR-4/NF-κB signaling pathway in synovial tissue of RA rats has been identified (Wang *et al*., 2023). Moreover, sitagliptin and tofacitinib modulate the JAK/STAT and TLR-4/NF-κB pathways to affect the progression of adjuvant arthritis (Wang *et al*., 2023). This study explored the significance of BMSCs in adjuvant-induced RA and their possible mechanisms via the JAK/STAT and TLR-4/NF-κB pathways, *in vitro* and *in vivo*.

**Corresponding author:* e-mail: xhzhouspine2024@126.com
#These authors contributed equally and are the co-first authors.

MATERIALS AND METHODS

Animals

A total of 40 SPF SD rats (6 weeks old, weighing 180–220 g, 20 males and 20 females) purchased from Beijing Vital River Laboratory Animal Technology Co., Ltd (Beijing, China; license No. SCXK (Jing) 2017-0011) were used in this study. All animals were housed under specific pathogen-free (SPF) conditions in a temperature-controlled room (22 ±2ºC) with a relative humidity of 50 – 60%. The animals were maintained on a 12-hour light/dark cycle (lights on from 07:00 to 19:00) and had ad libitum access to standard laboratory chow and autoclaved drinking water. Animals were housed in groups of 4 – 5 per cage (standard polycarbonate cages with wood chip bedding) and environmental enrichment (e.g., nesting material and tunnels) was provided to promote natural behaviors and reduce stress.All included rats were healthy, with no signs of infection or pre-existing joint abnormalities before the experiment. During the study, the following exclusion criteria were predefined: (1) animals that died during the experiment due to reasons unrelated to the treatments; (2) animals that failed to develop significant joint swelling and erythema (i.e., unsuccessful model induction) on the fourth day post-CFA injection. No animals or data points were excluded from the final analysis.

Cells

Fibroblast-like synovial MH7A cells, purchased from the Shanghai Chinese Academy of Sciences Cell Bank, were cultured in RPMI-1640 medium supplemented with 10% FBS in a 5% CO_2 incubator with saturated humidity at 37°C.

Drugs and reagents

Freund's complete adjuvant (CFA), Celastrol (Cel), cytoplasm and nuclear protein extraction kit and RT-qPCR kits were purchased from Beyotime Biotechnology; RPMI1640 medium, L-DMEM, PBS, FBS, penicillin mixture (100×), trypsin-EDTA digestion solution, CCK-8 kit, RIPA lysate, PMSF, skimmed milk powder, DAB color reagent, PVDF membrane from Beijing Solarbio Technology Co., Ltd.; IL- 6, IL-8 and TNF-α ELISA kits from Wuhan Elabscience Biotechnology Co., Ltd.; JAK2, p-JAK2, STAT3, p-STAT3, TLR4, P65, p-P65, lamin B, GAPDH monoclonal antibodies and goat anti-rabbit secondary antibody from CST (USA); Marker from SMOBiO company.

Apparatus

AE223 electronic balance was bought from Shanghai Sunny Hengping Instrument Co., Ltd.; By-dzc3000 electronic scale from Beijing Baoyuan Industrial Technology Co., Ltd.; MET VX200-T scroll oscillator from SHIRAY (Shanghai); DW-86L626 ultra-low temperature refrigerator from Haier Company; YA. ZD-10 ordinary electric distilled water device from Shanghai Shen'an Medical Instrument Factory; DYCZ-24KS dual-plate vertical electrophoresis instrument from Beijing Liuyi Instrument Factory; G : BOX multifunctional gel imaging system from Syngene; Multiskan MK3 microplate reader from Thermo Fisher Scientific; IX53 microscope from Olympus (Japan); TGL16MB high-speed refrigerated centrifuge from Changsha Xiangzhi Centrifuge Instrument Co., Ltd.; The open field device from Beijing Zhishu Duobao Biotechnology Co., Ltd.; the device for detection of thermal stimulation from Sichuan Keyicheng Technology Co., Ltd.

Animal grouping and model preparation

A total of 40 healthy SPF SD rats were randomly divided into 4 groups (n = 10 each): control, CFA, CFA + BMSC and CFA + Cel. The sample size (n = 10 per group) was determined based on a power analysis. Assuming an effect size of 0.8 for the primary outcome (serum TNF-α level) based on preliminary experiments, with a significance level (α) of 0.05 and a statistical power (1-β) of 0.80, a minimum of 8 animals per group was required. To account for potential dropouts, 10 animals were included in each group. This sample size is also consistent with previous studies using similar RA models and BMSC interventions (Pan *et al*., 2022; Liu *et al*., 2023).The literature documents that CFA can induce RA in rats (Liu *et al*., 2023). Briefly, the right anterior knee joint of the rat was disinfected and shaved, followed by injection of 0.1 ml CFA into the rat's knee joint for 3 consecutive days utilizing a syringe. On the fourth day, erythema and severe swelling of the rat's knee joint indicated successful modeling. Rats in the control group received an injection of saline and the procedure was the same as that of the modeled rats.

On the fifth day, rats in the CFA + BMSC group were injected with 15 mg/kg of BMSC via the tail vein, once every 3 days, for a total of 3 injections. The dosage and administration route of BMSCs were based on previous studies and this dosage has been proven to exert immunomodulatory effects in RA models (Pan *et al*., 2022). Rats in the CFA + Cel group were administered 2 mg/kg of Cel daily by gavage for 9 consecutive doses. Cel, used as a positive control drug (administered at a dose of 2 mg/kg), has been shown to alleviate RA symptoms through its anti-inflammatory effects (Liu *et al*., 2023). The control and CFA groups received normal saline (same volume) daily.All animals were monitored daily for signs of pain, distress and general health throughout the experiment. A humane endpoint scoring system was established to minimize suffering, with predefined criteria for early euthanasia, including: (1) severe, persistent lethargy or inability to reach food/water; (2) rapid weight loss exceeding 20% of initial body weight; (3) severe joint swelling or ulceration that significantly impaired mobility. In this study, no animals met these early termination criteria. For pain management, all rats were closely monitored and those exhibiting significant pain-related

behaviors were immediately euthanized.No additional analgesics were administered during the study to avoid interference with the inflammatory model and experimental outcomes.

Determination of thermal pain threshold

A thermal stimulation device was used to measure paw withdrawal thermal latency (PWTL) to assess heat sensitivity and pain in rats. When the rat is in a freely active state, the rat's left hind limb was placed on the device, with the stimulus intensity set to IR = 72. The reaction time was recorded when the rat paw moved, that is, the PWTL at the bottom of the rat's foot.

Behavioral testing

The open-field device measured 80 cm × 80 cm × 60 cm. The experiment was carried out in a relatively dark environment. During the experiment, the rat was gently placed in the center of the open field and acclimated for 5 min, followed by imaging of the rat's spontaneous activity (recorded continuously for 5 min). The total distance of the rats' spontaneous movements was analyzed. An automatic gait analysis system was used for testing, with a conveyor belt speed of 12 cm/s and a shutter speed for photographing of 40 m/s. Each animal was recorded for 6 seconds. Before the end of the experiment, rats were trained for 3 days continuously, once a day and each animal ran for 1 minute each time. After 9 days of continuous administration of BMSC or Cel, the test began and the DigiGait software was used to automatically recognize paw footprints for analyzing gait parameters such as step length, step width and forelimb angle changes.

Collection of blood and tissue samples

After the above experiment, blood was collected from the eyes of the rats and the supernatant was obtained after centrifugation (3000 r/min) for 10 min and preserved at −20°C for subsequent experiments. After that, the rats were sacrificed and a longitudinal incision was made along the right knee joint to collect synovial tissue, which was then immediately placed in an RNase-free centrifuge tube and preserved at −80°C.

ELISA

The blood sample was chose for checking the serum levels of TNF-α, IL-8 and IL-6 in strict accordance with the ELISA kit instructions.

RT-qPCR

Trizol was used for total RNA extraction from synovial tissue and the RNA was reverse-transcribed into cDNA, followed by RT-qPCR amplification. Reaction system (20 μL) was: 2 μL of cDNA (200 ng/μL), 10 μL of SYBR® Premix ExTaqTM (2×), 0.4 μL of upstream primer and 0.4 μL of downstream primer and 7.2 μL of ddH_2O. Reaction conditions were pre-denaturation at 94°C for 10 min, denaturation at 95°C for 15 s, annealing at 60°C for 20 s and extension at 75°C for 20 s (40 cycles). Using GAPDH as the loading control, the 2-ΔΔCt method was used to calculate the fold change.

Western blot assay

Frozen synovial tissue was used to determine the protein expression of STAT3, p-STAT3, nuclear NF-κB p65, p-IκB-α and IκB-α using western blot assay. A nuclear protein extraction kit was used to extract nuclear protein (for NF-κB p65 protein level). The remaining cells were lysed in protein lysis buffer on ice for 10 min, then centrifuged at 10,000 r/min for 10 min. The collected supernatant is the total protein (for other proteins). The protein was separated by gel electrophoresis and transferred to PVDF membrane which was reacted with 5% skimmed milk powder for 2 h and reacted with anti-JAK2, p-JAK2, STAT3, p-STAT3, TLR4, P65, p-P65, lamin B (internal reference for nuclear protein) and GAPDH (internal reference for the remaining proteins) overnight at 4°C. Then, the membrane was reacted with the corresponding Ⅱ antibody for 1 h and developed with a DAB color development kit in the dark. The protein gel imager was used for imaging and the gel image processing system was used for analyzing gray values.

Isolation and culture of BMSCs

The rats were sacrificed, immersed in 75% ethanol solution for 10 min and washed with 0.9% sodium chloride solution. Then, bilateral tibia and femur were separated under an ultra-clean table and both epiphyses were cut off. The bone marrow cavity was rinsed with PBS 3 to 5 times until it turned white, then placed in a centrifuge tube for thorough pipetting. The sample was filtered through a 100 μm cell sieve, centrifuged at 1,500 r/min for 5 min with the supernatant discarded, resuspended in L-DMEM containing 10% FBS and 1% penicillin and pipetted again to make a single-cell suspension. Cell suspension was inoculated into a 37°C, 5% CO_2 cell incubator with medium changed every other day. Upon 70% confluency, cells were digested by trypsin and passaged. After being cultured *in vitro to the third passage,* cell surface markers were detected by flow cytometry. The results showed that the positive expression rates of CD73, CD90 and CD105 were all >95%, while the negative expression rates of CD34 and CD45 were <2%, consistent with the typical immunophenotypic characteristics of BMSCs.

Co-culture of MH7A cells and BMSCs

MH7A cells were placed in culture flasks (3 × 10^5/mL) and then divided into control, CFA + MH7A and BMSC + MH7A groups. In the CFA + MH7A group, cells were treated with 20 ng/ml CFA; in the BMSC + MH7A group, cells were stimulated with 20 ng/ml CFA to simulate an inflammatory environment. Co-culture was conducted at a cell ratio of BMSC: MH7A = 1:10. Cell incubation was implemented with RPMI-1640 medium appended to 10% FBS and 1% penicillin double antibody in a 37°C, 5% CO_2 cell incubator.

Table 1: Comparison of gait parameters of each group ($\bar{x} \pm s$).

Group	Step length (cm)	Step width (cm)	Swing time (s)	Time to bottom (s)
Control	8.52±0.31	3.31±0.33	0.102±0.002	0.122±0.007
CFA	4.20±0.61*	4.87±0.19*	0.061±0.003*	0.181±0.004*
CFA + BMSC	7.74±0.61#	3.50±0.49#	0.08±0.041#	0.158±0.023#
CFA + Cel	7.86±0.53#	4.01±0.32#	0.076±0.008	0.172±0.062

Note: Compared with the control group, *p < 0.05; compared with the CFA group, #p < 0.05.

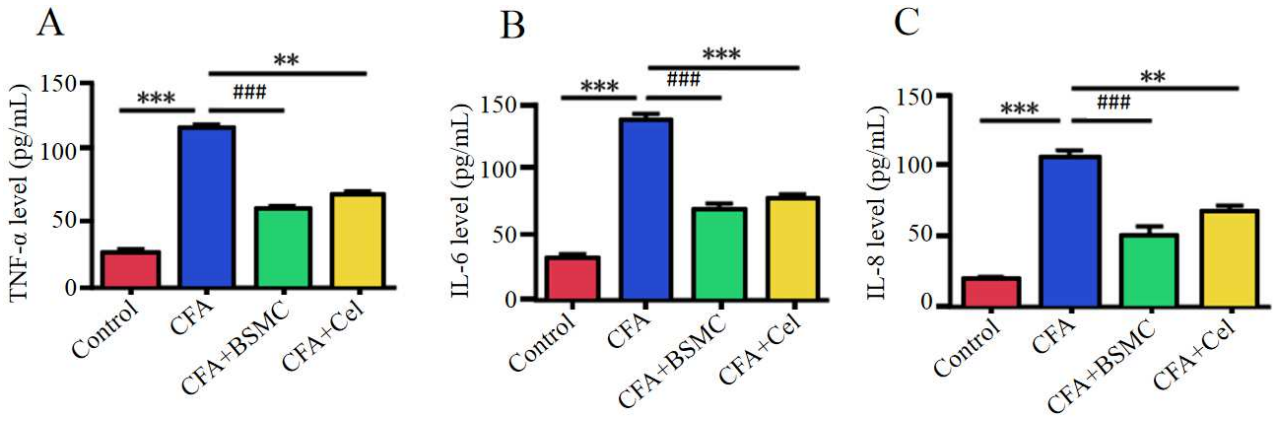

Fig. 1: ELISA method to detect the contents of TNF-α, IL-6 and IL-8 in serum of each group (pg/mL).
Note: (A) TNF-α; (B) IL-6; (C) IL-8. Control group vs. CFA group, ***p < 0.001; CFA group vs. CFA + BMSC group, ###p < 0.001; CFA group vs. CFA + Cel group, **p < 0.01, ***p < 0.001.

CCK-8 assay

The MH7A cells were digested, resuspended and calculated and then placed in a 96-well plate (8000 cells/well). Following incubation in a CO_2 incubator for 48 h, 100 μL of CCK8 mixture was added for another 2-h of incubation. An enzyme-linked immunoassay was chose to detect the absorbance (A450 nm) value.

Detection of cytokine levels in co-culture supernatant

After 24 h of co-cultivation, the culture supernatant was drawn separately and the content of IL-6, IL-8 and TNF-α in the supernatant was detected by ELISA.

Detection of related protein expression in co-culture condition

The cytoplasm and nucleoprotein extraction kit was employed to extract MH7A cytoplasmic protein and nuclear protein to detect related protein levels. The remaining cells were lysed utilizing protein lysis buffer for 10 min, centrifuged (10,000 r/min) for 10 min and the collected supernatant was total protein (for the remaining protein levels). The specific procedures were the same as we mentioned in Western bolt assay section.

Statistical processing

SPSS23.0 statistical software was chose for data analysis, the measurement data was summarized in ($\bar{x} \pm s$). One-way analysis of variance and SNK-q test were chose for data comparison. The difference was concluded as statistically significant with $p < 0.05$.To minimize bias, the experimenters responsible for animal assignment, treatment administration, behavioral testing, molecular analysis and statistical analysis were all blinded to the group allocations throughout the entire study. The codes for group allocation were only broken after all data analyses were completed.

RESULTS

Comparison of PWTL of each group

The PWTL values in the control, CFA group, CFA + BMSC group and CFA + Cel groups were (17. 31 ± 2. 06) s, (6. 64 ± 0.88) s, (12 ± 2. 04) s, (12. 07 ± 1.81) s, respectively. Significance was seen in comparison between CFA and control groups as well as between CFA + BMSC and CFA + Cel groups with CFA group ($p < 0.05$).

Comparison of gait parameters in each group

The gait parameters are shown in table 1. The step length and step width of the rats in the CFA group increased and the swing time decreased (p < 0.05 vs. the control group). Relative to CFA group, the step length of rats in the CFA + BMSC and CFA + Cel groups was increased (p <0. 05) and the step width was declined (p <0. 05).

Detection of TNF-α, IL-6 and IL-8 levels in serum

ELISA results showed significantly elevated serum levels of TNF-α, IL-6 and IL-8 in the CFA group (p < 0.001 vs. the control group). Compared with the CFA group, declines were observed in the above factors in the CFA + BMSC group (p < 0.001). Moreover, relative to CFA group, the afore-mentioned factors in the CFA + Cel group were declined ($p < 0.01$ for TNF-α and IL-8 levels, $p < 0.001$ for IL-6) (Fig. 1).

Table 2: RT-qPCR detection of JAK/STAT and TLR-4/NF-κB signaling pathway-related genes in synovial tissues.

Group	JAK2	STAT3	TLR4	NF-κB P65
Control	0.92±0.19	0.89±0.05	0.09±0.18	0.78±0.02
CFA	1.97±0.31*	1.93±0.07*	2.99±0.09 *	1.23±0.04*
CFA + BMSC	0.55±0.42*	0.45±0.05*	0.84±0.08*	0.76±0.22*
CFA + Cel	1.55±0.53	1.48±0.10	1.63±0.07	1.20±0.15

Note: Compared with the control group, *p <0.05.

Table 3: Western blot detection of JAK/STAT and TLR-4/NF-κB pathway-related proteins in synovial tissues.

Group	JAK2/p-JAK2	STAT3/p-STAT3	TLR4	P65/p-P65
Control	100.90 ± 7.50	99.22 ± 1.41	100.14 ± 0.02	103.22 ± 6.57
CFA	217.60 ± 18.14*	316.70 ± 40.92*	150.52 ± 0.05*	173.27 ± 8.50*
CFA + BMSC	122.00 ± 11.06#	150.22 ± 1.41#	120.26 ± 0.03#	116.92 ± 7.67#
CFA + Cel	147.32 ± 4.72	208.73 ± 4.95	130.37 ± 0.04	144.76 ± 5.49

Note: Compared with the control group, *p < 0.05, compared with the CFA group, #p < 0.05.

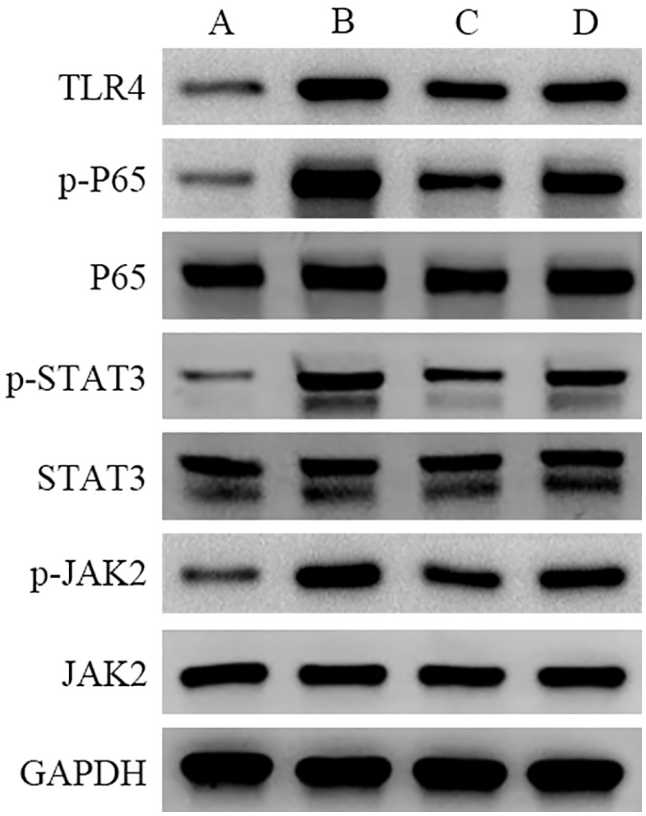

Fig. 2: Western blot detection of protein expression levels of JAK/STAT and TLR-4/NF-κB pathway-related proteins in rat synovial tissue of each group.
Note: (A) Control group; (B) CFA group; (C) CFA + BMSC group; (D) CFA + Cel group. GAPDH was used as an internal control.

Expression of JAK/STAT and TLR-4/NF-κB pathway-related genes in synovial tissues

RT-qPCR results clarified that relative to the control group, the expression of JAK2, STAT3, TLR4 and P65 mRNA in the CFA group was increased ($p < 0.05$), while opposite trends were seen in the CFA + BMSC group ($p < 0.05$) (Table 2).

Western blot detection of JAK/STAT and TLR-4/NF-κB pathway-related proteins in synovial tissues

As reflected in table 3 and figure 2, relative to the control group, enhancement in the relative expression of JAK2, p JAK2, STAT3, pSTAT3, TLR4 and P65/p-P65 was seen in the CFA group ($p <0.05$); in comparison with CFA group, declines were observed in the above-mentioned proteins in the CFA + BMSC group.

The aforesaid results pinpointed that BMSC limited the phosphorylation of JAK2, STAT3 and P65 protein, as well as the expression of TLR4.

Effect of BMSC on the viability of MH7A cells

Co-culture with BMSCs significantly reduced MH7A cell viability ($p < 0.001$ vs. control or CFA + MH7A group) (Fig. 3).

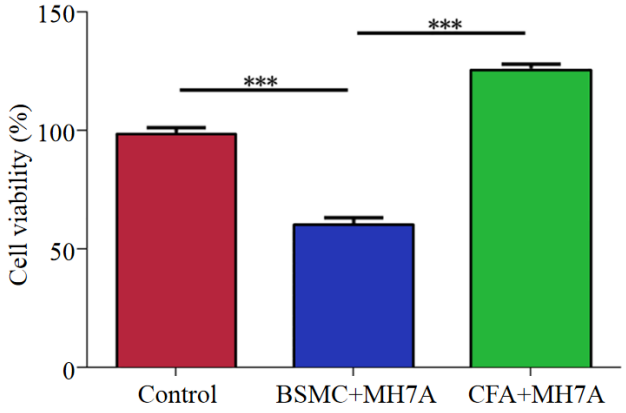

Fig. 3: CCK-8 assay for detecting MH7A cell viability after 24 hours of co-culture in each group.
Note: Control group and CFA + MH7A group vs. BMSC + MH7A group, ***p < 0.001.

Detection of cytokine levels in the co-culture supernatant

ELISA showed that after 24 h of co-culture, the TNF-α, IL-6 and IL-8 levels in the cell culture supernatant of BMSC + MH7A group were diminished ($p < 0.001$ vs. control group); the above levels were rose in CFA + MH7A group ($p < 0.001$ vs. BMSC + MH7A group) (Figure 4), indicating that BMSC can inhibit the release of inflammatory factors from MH7A cells.

Determination of JAK/STAT and TLR-4/NF-κB pathway-related proteins under co-culture condition

After co-culture for 24 h, we found elevated expression of JAK2, p-JAK2, STAT3, p-STAT3, TLR4 and P65/p-P65 proteins in CFA group ($p < 0.05$ vs. control group). In comparison to CFA + MH7A group, the above protein expression was declined in BMSC + MH7A cells group ($p < 0.05$) (Table 4, Fig. 5). These results indicated that BMSCs inhibited the phosphorylation of JAK2, STAT3 and P65, as well as the expression of TLR4.

DISCUSSION

RA is a chronic autoimmune disease characterized by persistent synovitis and progressive bone destruction in multiple joints. The main clinical manifestations of the sufferers are progressive erosive arthritis and morning stiffness and some patients also have external manifestations such as fever, subcutaneous nodules and lymphadenopathy (Yaman *et al*., 2025; Gupta *et al*., 2025). At the molecular and pathophysiological levels, RA is characterized by abnormalities in innate, cellular and humoral immunity (Jiang *et al*., 2022; Cui *et al*., 2022). The immune abnormalities in the pathogenesis of RA can lead to abnormal activation of T lymphocytes, B lymphocytes, neutrophils, macrophages and synovial tissue fibroblasts, which are the main cell markers of the RA disease process (Cai and Yao, 2025; Zheng *et al*., 2025).

BMSCs can improve immune regulation in autoimmune diseases and have been shown to exert therapeutic effects in multiple sclerosis (Wang *et al*., 2024; Xiu *et al*., 2025), RA (Wang *et al*., 2025; Gao *et al*., 2025) and other immune diseases. El-Sayed *et al*. (2026) reported that BMSCs ameliorate bone erosion in collagen-induced arthritis by inhibiting bone-healing-related factors and chondrocyte differentiation. Researchers found that BMSCs repaired joint damage *in vitro* after inoculating BMSCs into nano-hMSCs in CIA rats (El-Sayed *et al*., 2025). In addition, evidence highlighted the crucial role of increased levels of various pro-inflammatory cytokines in the development of rheumatoid arthritis and these cytokines may lead to the destruction of articular cartilage and erosion of subchondral bone (Cheon *et al*., 2024; Andreev *et al*., 2025).

We also identified the regulatory effects of BMSCs on RA using *in vitro* and *in vivo* assays. *In vitro, we first isolated BMSCs, then co-cultured them with MH7A cells and detected related inflammatory marker*s. *In vivo, we constructed a rat RA model via CFA induction, followed by BMSC injection to test PWTL and gait parameters, as well as* related inflammatory factors. The results showed that BMSCs reduced the symptoms of CFA-induced arthritis in rats and effectively inhibited the expression of inflammatory factors, demonstrating the therapeutic effects of BMSCs on RA both *in vitro* and *in vivo*. As previously reported, a variety of pathways play a role in the development of RA. For example, crosstalk between SAPK/MAPK and PI3K/Akt/mTOR pathways has been shown to be associated with abnormal survival of both non-immune and immune cells in RA (Cheng *et al*., 2022). Accumulating evidence indicates that the JAK/STAT pathway accelerates RA progression by driving chronic inflammation (Kung *et al*., 2025; Liu *et al*., 2025). For example, microRNA-17-5p directly targets the JAK/STAT pathway to limit inflammation and bone erosion in RA mice (Chang *et al*., 2022). More importantly, targeting JAK proteins has been successful in clinical trials and some JAK inhibitors, such as tofacitinib, have been shown to be effective in treating RA (Mikaeili *et al*., 2025; Lee *et al*., 2025). In addition, moxibustion treatment can limit TLR4/NF-κB signal transduction in the synovial tissue of the ankle joint, thereby reducing ankle joint swelling in RA rats (Kun *et al*., 2024). Compared with existing JAK inhibitors or NF-κB pathway inhibitors, the advantage of BMSCs lies in their multi-target regulatory capacity.

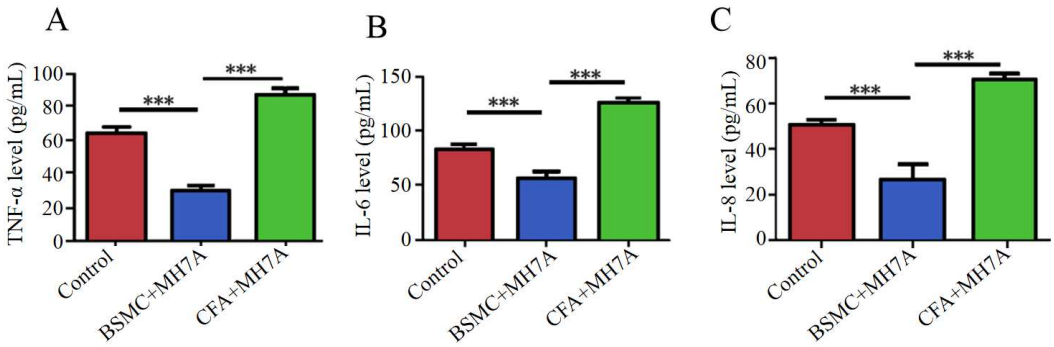

Fig. 4: ELISA detection of TNF-α, IL-6 and IL-8 levels (pg/mL) in cell culture supernatants after 24 hours of co-culture in each group.
Note: Control group and CFA + MH7A group vs. BMSC + MH7A group, ***p < 0.001.

Table 4: Western blot detection of JAK/STAT and TLR-4/NF-κB pathway-related proteins under co-culture condition.

Group	JAK2/p-JAK2	STAT3/p-STAT3	TLR4	P65/p-P65
Control	22.34 ± 5.85	13.20 ± 1.80	9.00 ± 0.02	14.76 ± 0.48
CFA + MH7A	73.92 ± 9.61*	63.05 ± 5.70*	13.420 ± 0.16*	15.45 ± 2.45*
BMSC + MH7A	50.26 ± 2.90#	52.73 ± 12.32#	12.110 ± 0.09#	18.15 ± 3.49#

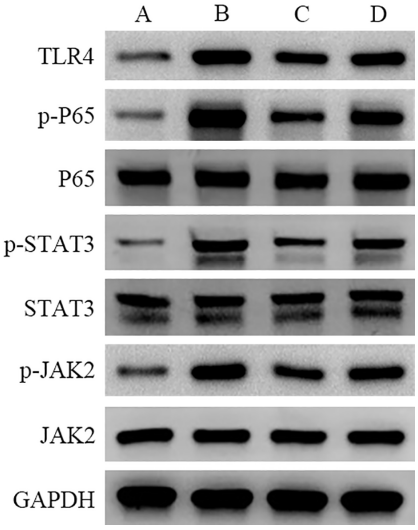

Fig. 5: Western blot detection of protein expression levels of JAK/STAT and TLR-4/NF-κB pathway-related proteins under co-culture conditions.
Note: (A) Control group; (B) CFA + MH7A group; (C) BMSC + MH7A group. GAPDH was used as an internal control.

JAK inhibitors primarily target the JAK/STAT pathway; although they can effectively suppress inflammation, long-term use may pose risks of infection and adverse effects related to immunosuppression (Jarneborn *et al*., 2025). In contrast, BMSCs not only simultaneously regulate two key pathways—JAK/STAT and TLR-4/NF-κB—but also possess multiple advantages, including immunomodulation, tissue repair and low immunogenicity, demonstrating a more comprehensive therapeutic potential (Ru *et al*., 2023; Swierczek-Lasek *et al*., 2022). Furthermore, as living cell preparations, BMSCs can exert sustained effects *in-vivo*, offering the prospect of more durable and stable therapeutic outcomes. To investigate the molecular mechanism of BMSCs in RA, we examined the expression of factors related to the JAK/STAT and TLR-4/NF-κB pathways *in-vitro* and *in-vivo*. The results showed that BMSCs decreased the relative expression of JAK2, p-JAK2, STAT3, pSTAT3, TLR4, P65 and p-P65. The aforesaid findings concluded that the therapeutic action of BMSCs in RA was achieved by blocking the JAK/STAT and TLR-4/NF-κB pathways.

However, this study has several limitations. First, it focused primarily on the regulatory effects of BMSCs on inflammatory responses, without thoroughly exploring their potential roles in cartilage repair or in inhibiting bone erosion. Second, the crosstalk mechanism between the JAK/STAT and TLR-4/NF-κB pathways has not been fully elucidated and whether BMSCs coordinately regulate these two pathways through intermediary molecules remains to be investigated. Additionally, this study did not compare the efficacy and safety of BMSCs with those of existing JAK inhibitors. Future studies may establish a positive control drug group to evaluate the clinical application value of BMSCs further. Subsequent research can combine gene knockouts and pathway-specific agonists or inhibitors to explore the regulatory mechanisms of BMSCs within multi-pathway networks deeply and to investigate the optimal administration regimen and long-term safety of BMSCs in the treatment of RA.

CONCLUSION

In conclusion, this study found, through *in vitro* co-culture experiments, that BMSCs significantly inhibited the release of inflammatory cytokines in MH7A cells and downregulated the expression of JAK2, p-JAK2, STAT3,

p-STAT3, TLR4, P65 and p-P65. In the CFA-induced rat model of RA, BMSCs similarly reduced inflammatory cytokine levels and improved paw withdrawal thermal latency (PWTL) and gait parameters induced by thermal stimulation. These results indicate that BMSCs effectively alleviate RA-associated inflammation at both cellular and animal levels by blocking the JAK/STAT and TLR-4/NF-κB signaling pathways. This study provides new experimental evidence for the application of BMSCs in the treatment of RA. However, this study focused only on the inflammatory response; whether BMSCs can also exert functions in RA by regulating other proteins or signaling pathways remains to be further researched.

Acknowledgments
We gratefully acknowledge the Shanghai Changzheng Hospital for providing the necessary equipment for this study.

Author's contributions
Shilin Lian and Xiao Ma contributed equally to this work and share first authorship. Shilin Lian contributed to conceptualization, methodology, investigation, data curation, formal analysis and writing of the original draft. Xiao Ma contributed to investigation, validation, visualization and data curation. Yichen Meng contributed to methodology, formal analysis and writing–review and editing. Xuhui Zhou contributed to supervision, project administration, funding acquisition and writing–review and editing. All authors read and approved the final manuscript.

Funding
This study was supported by the National Natural Science Foundation of China (Grant No. 82372360).

Data availability statement
The datasets generated during and/or analysed during the current study are available from the corresponding author on reasonable request.

Ethical approval
This study was approved by the Animal Ethics Committee of Shanghai Changzheng Hospital (Approval No. : 2025SL1899). This study was performed in adherence with the ARRIVE guidelines. See supplementary file for the ARRIVE checklist.

Conflict of interest
The authors declare that they have no conflict of interest.

Supplementary data

REFERENCES

Andreev D, Porschitz P, Weidner D, Song R, Weider M, Schett G, Golz L and Bozec A (2025). A multidimensional analysis of temporomandibular joint and ankle joint erosion in inflammatory arthritis. *Front Immunol*., **16**: 1560723.

Chen K, Chen X, Huang S, Zhou L, Zhou X, Lu Y and Feng Z (2025). Therapeutic effects and mechanisms of Tripterygium wilfordii extracts in rheumatoid arthritis: A systematic review and meta-analysis of preclinical studies. *Sci Rep*., **15**(1): 27960.

Cui L, Weiyao J, Chenghong S, Limei L, Xinghua Z, Bo Y, Xiaozheng D and Haidong W (2022). Rheumatoid arthritis and mitochondrial homeostasis: The crossroads of metabolism and immunity. *Front Med (Lausanne)*., **9**: 1017650.

Cai X and Yao Y (2025). Epigenetic modifications of immune cells in rheumatoid arthritis. *Ann Med*., **57**(1): 2533432.

Cheon YH, Lee CH, Eun SY, Park GD, Chung CH, Kim JY and Lee MS (2024). Vigeo attenuates cartilage and bone destruction in a collagen-induced arthritis mouse model by reducing production of pro-inflammatory cytokines. *Exp Ther Med*., **27**(5): 208.

Cheng Q, Chen M, Liu M, Chen X, Zhu L, Xu J, Xue J, Wu H and Du Y (2022). Semaphorin 5A suppresses ferroptosis through activation of PI3K-AKT-mTOR signaling in rheumatoid arthritis. *Cell Death Dis*., **13**(7): 608.

Chang C, Xu L, Zhang R, Jin Y, Jiang P, Wei K, Xu L, Shi Y, Zhao J, Xiong M, Guo S and He D (2022). MicroRNA-mediated epigenetic regulation of rheumatoid arthritis susceptibility and pathogenesis. *Front Immunol*., **13**: 838884.

Deng Y, Yuan D, Deng Z, Liang J, Zhang Z, Hei Z and Li X (2023). Bone marrow-derived mesenchymal stem cells attenuate complete Freund's adjuvant-induced inflammatory pain by inhibiting the expression of P2X3. *Cell Prolif*., **56**(10): e13461.

El-Sayed SM, Mohamed MR, Naguib MM, Aglan HA and Ahmed HH (2026). Hydrogen sulphide modifies the therapeutic potential of bone marrow mesenchymal stem cells in an adjuvant-induced polyarthritis rat model through the mitigation of angiogenesis, ectopic lymphoid tissue formation and osteoclastogenesis. *Inflammopharmacology*., **34**(1): 399–418.

El-Sayed SM, Ahmed HH, Aglan HA, Naguib MM and Mohamed MR (2025). Preconditioning of bone marrow mesenchymal stem cells with sodium hydrosulfide enhances their therapeutic potential in type II collagen-induced arthritis rat model. *Naunyn Schmiedebergs Arch Pharmacol*., **398**(11): 15645–15663.

Guzel Erdogan D, Demır A, Baylan H, Budak O, Cokluk E and Tanyerı P (2025). Effects of different doses of Ganoderic Acid A on nociceptive behaviour and inflammatory parameters in polyarthritic mice rheumatoid arthritis model. *Sci Rep*., **15**(1): 15759.

Gupta A, Anis S and de Pablo P (2025). Imaging tests as predictors of progression to rheumatoid arthritis in

clinically suspect arthralgia: A systematic review and meta-analysis. *Rheumatology (Oxford)*., **64**(6): 3255–3265.

Gao YF, Zhao N and Hu CH (2025). Harnessing mesenchymal stem/stromal cells-based therapies for rheumatoid arthritis: Mechanisms, clinical applications and microenvironmental interactions. *Stem Cell Res Ther*., **16**(1): 379.

Hu Q, Bian Q, Rong D, Wang L, Song J, Huang HS, Zeng J, Mei J and Wang PY (2023). JAK/STAT pathway: Extracellular signals, diseases, immunity and therapeutic regimens. *Front Bioeng Biotechnol*., **11**: 1110765.

Jing W, Liu C, Su C, Liu L, Chen P, Li X, Zhang X, Yuan B, Wang H and Du X (2023). Role of reactive oxygen species and mitochondrial damage in rheumatoid arthritis and targeted drugs. *Front Immunol*., **14**: 1107670.

Jiang SZ, To JL, Hughes MR, McNagny KM and Kim H (2022). Platelet signaling at the nexus of innate immunity and rheumatoid arthritis. *Front Immunol*., **13**: 977828.

Jarneborn A, Kopparapu PK and Jin T (2025). The dual-edged sword: Risks and benefits of JAK inhibitors in infections. *Pathogens*., **14**(4): 324.

Kiełbowski K, Plewa P, Bratborska AW, Bakinowska E and Pawlik A (2024). JAK inhibitors in rheumatoid arthritis: Immunomodulatory properties and clinical efficacy. *Int J Mol Sci*., **25**(15): 8327.

Kung SP, Umbreen H, Wang JH, Tsia CM, Lin TC and Chen YT (2025). Cucurbitacin B inhibits Th17 cell differentiation via the suppression of the JAK/STAT pathway and alleviates collagen-induced arthritis in mice. *Int J Immunopathol Pharmacol*., **39**: 3946320251348715.

Kun L, Yumei Z, Yanding G, Linlin Z, Danhui HU, Wenbin MA, Xin Y and Haiyan Z (2024). Moxibustion inhibits the macrophage M1 polarization toll-like receptor 4/myeloid differentiation factor 88/nuclear factor kappa B signaling pathway by regulating T-cell immunoglobulin and mucin-containing protein-3 in rheumatoid arthritis. *J Tradit Chin Med*., **44**(6): 1227–1235.

Liu J, Zhao N, Su SH, Gao Y and Qi B (2023). Anti-arthritic effect of edaravone against complete freund adjuvant induced arthritis via osteoclast differentiation and HIF-1α-VEGF-ANG-1 axis. *Drug Des Devel Ther*., **17**: 519–534.

Liu H, Li Q, Chen Y, Dong M, Liu H, Zhang J, Yang L, Yin G and Xie Q (2025). Suberosin attenuates rheumatoid arthritis by repolarizing macrophages and inhibiting synovitis via the JAK/STAT signaling pathway. *Arthritis Res Ther.*, **27**(1): 12.

Lee YJ, Choi G, Yeo J, Baek J, Choi H, Kim M, Kim YG, Kim BY and Koo J (2025). Machine learning-based prediction of response to Janus kinase inhibitors in patients with rheumatoid arthritis using clinical data. *Front Immunol*., **16**: 1689144.

Liu D, Liu Y, Qian X, Yang J, Li C, Zhu L and Zhou J (2023). Pharmacokinetic study on the effect of ligustrazine-tangeretin co-administration on the pharmacokinetics of ligustrazine and its potential mechanism in rats. *Pharmacol Res Perspect*., **11**(2): e01058.

Mikaeili B, Alqahtani ZA, Hincapie AL and Guo JJ (2025). Safety of Janus kinase inhibitors in rheumatoid arthritis: A disproportionality analysis using FAERS database from 2012 to 2022. *Clin Rheumatol*., **44**(4): 1467–1474.

Pan C, Lu F, Hao X, Deng X, Liu J, Sun K, Hou W, Shang X, Chi R, Guo F and Xu T (2024). Low-intensity pulsed ultrasound delays the progression of osteoarthritis by regulating the YAP-RIPK1-NF-κB axis and influencing autophagy. *J Transl Med*., **22**(1): 286.

Pan S, Wang L, Wu B and Xing H (2022). Effect and mechanism of siRNAs targeting IL-1β/TNF-α combined with BMSCs transplantation in ameliorating rheumatoid arthritis in rats. *Vet Sci*., **9**(10): 531.

Ru X, Cai P, Tan M, Zheng L, Lu Z and Zhao J (2023). Temporal transcriptome highlights the involvement of cytokine/JAK/STAT3 signaling pathway in the osteoinduction of BMSCs. *J Orthop Surg Res*., **18**(1): 289.

Swierczek-Lasek B, Tolak L, Bijoch L, Stefaniuk M, Szpak P, Kalaszczynska I, Streminska W, Ciemerych MA and Archacka K (2022). Comparison of muscle regeneration after BMSC-conditioned medium, syngeneic, or allogeneic BMSC injection. *Cells*, **11**(18): 2843.

Wen J, Liu J, Wan L and Wang F (2023). Long noncoding RNA/circular RNA regulates competitive endogenous RNA networks in rheumatoid arthritis: Molecular mechanisms and traditional Chinese medicine therapeutic significances. *Ann Med*., **55**(1): 973–989.

Wang X, Liu D, Li D, Yan J, Yang J, Zhong X, Xu Q, Xu Y, Xia Y, Wang Q, Cao H and Zhang F (2023). Combined treatment with glucosamine and chondroitin sulfate improves rheumatoid arthritis in rats by regulating the gut microbiota. *Nutr Metab (Lond)*., **20**(1): 22.

Wang R, Li Y, Liu Y, Hou X and Li C (2023). Synovitis, acne, pustulosis, hyperostosis and osteitis (SAPHO) syndrome with henoch-schonlein purpura: A case report. *Clin Cosmet Investig Dermatol*., **16**: 1089–1094.

Wang S, Zhang K, Wang L and Guo Y (2025). Stem cell-derived exosomes with high expression of PD-L1 as nanotherapeutics in rheumatoid arthritis model mice. *Int J Nanomedicine*., **20**: 8935–8949.

Xiu X, Chen S, Liu Y, Sun B, Li H, Zhang S, Yang X, Wei Y, Peng X, Wang Y, Wang Y, Wu J, Zhang Y, Mu L, Kong Q and Liu X (2025). Synergistic potential of bone marrow mesenchymal stem cells and miR181-a combinational therapy against multiple sclerosis. *Stem Cell Res Ther*., **16**(1): 300.

Yaman R, DiCaudo DJ, Sokumbi O, Pham MM, Aslam F, Griffing WL and Sullivan MM (2025). Cutaneous

nodules and inflammatory arthritis: Two illustrative cases of rare mimics of rheumatoid arthritis. *J Clin Med*., **14**(14): 4940.

Zhang Y, Cao XQ, Ma XL, Guo YY, Zhang T, Wu LL, Yang YS, Hao CF, Liu WL and Guo JT (2025). RNA binding protein YTHDF2 inhibits synovial fibroblast inflammation and bone injury in rheumatoid arthritis by reducing the mRNA stability of IL-6R. *Kaohsiung J Med Sci*., **41**(8): e70010.

Zhang X, Fu X, Chen W, Chen P, Zhu H, Yang B, Liang J and Zeng F (2025). Amelioration of the rheumatoid arthritis microenvironment using celastrol-loaded silver-modified ceria nanoparticles for enhanced treatment. *J Nanobiotechnology*., **23**(1): 372.

Zheng S, Wang H, Mu J, Liu X, Jin X, Li Z, Jiang J and Yang M (2025). Macrophage-centred crosstalk with infiltrating immune cells in rheumatoid arthritis and its regulation by mesenchymal stem cells. *J Transl Med*., **23**(1): 1360.

Wang Y, Xiao Y, Yang X, He F, Hu J, Yang G and Wang W (2024). Bone marrow mesenchymal stem cells overexpressing stromal cell- derived factor 1 aid in bone formation in osteoporotic mice. *BMC Musculoskelet Disord*., **25**(1): 878.